ELSEVIER

Polymer 43 (2002) 3359–3364

polymer

www.elsevier.com/locate/polymer

Control of mesh pattern of surface corrugation via rate of solvent evaporation in solution casting of polymer film in the presence of convection

Shinichi Sakurai*, Chizuko Furukawa, Akihiko Okutsu, Akira Miyoshi, Shunji Nomura

Department of Polymer Science and Engineering, Kyoto Institute of Technology, Matsugasaki, Sakyo-ku, Kyoto 606-8585, Japan

Received 9 May 2001; received in revised form 30 November 2001; accepted 18 February 2002

Abstract

A polygonal mesh pattern was observed on an as-cast polymer film when cast from a dilute solution on a hot plate. It was found that the pattern was ascribed to surface corrugation. In the dilute solution, a similar polygonal mesh pattern due to convection was present. A possible imprinting mechanism of the convection pattern on the as-cast polymer film as the surface corrugation was investigated by real time observation using the so-called shadowgraph technique. For this purpose poly(styrene-*ran*-butadiene) random copolymer was used as a solute and toluene as a solvent. Furthermore, control of the mesh size via the rate of solvent evaporation was examined. It was found that the mesh size was increased with an increase of the rate in the regime of the lower evaporation-rate (regime I) and that it was decreased tremendously with an increase of the rate in the regime of the higher evaporation-rate (regime II). These regimes can be referred to as a kinetic control regime and a temperature-gradient control regime, respectively.

Keywords: Mesh pattern; Polymer film; Surface corrugation

1. Introduction

Dissipative structures are fascinating fabrications formed at a state far from equilibrium [1–6]. The dissipative structure gives rich phenomena of a pattern formation problem [7] and has been attracting interests since many decades ago [3]. One example is a set of patterns due to convection in a thin layer of fluid [1–6]. Recently, fluid containing polymeric materials is becoming a target of research [8–14] because formation of dissipative structures can be applied to a novel control technique for producing new functional polymeric materials [15]. As a matter of fact, convective flows were found to be effective for self-organization of domains in phase separating polymer blends [12]. For polymer solutions, one of the simplest applications of convection is patterning of surface corrugation [8–11,13]. A polygonal mesh pattern due to surface corrugation was observed on an as-cast polymer film when cast from a dilute solution on a hot plate in the presence of convection [9]. It was considered that a polygonal mesh pattern due to convection in the dilute solution was imprinted on the as-cast polymer film as the surface corrugation. The present study is intended to experimentally elucidate a possible imprinting mechanism and further to control the size of the surface corrugation pattern by controlling the rate of solvent evaporation.

The convection relevant to this study is the Bénard–Marangoni (BM) convection [4] where force driven by inhomogeneity in surface tension couples with buoyancy due to thermal expansion. Note that the latter causes ordinary thermal convection, which is referred to as the Rayleigh–Bénard (RB) convection [1–6].

2. Experimental section

The sample used was poly(styrene-*ran*-butadiene) random copolymer (SBR-0202, Japan Synthetic Rubber). The number-average molecular weight, M_n, is 1.5×10^5 (by GPC), the heterogeneity index for the molecular weight distribution, M_w/M_n, is 3.1, and the weight fraction of polystyrene (PS), w_{PS}, is 0.46 (by FTIR), where M_w denotes the weight-average molecular weight. The microstructure of the butadiene moiety was analyzed by FTIR to be 21% *cis*-1,4, 27% *trans*-1,4, and 6% 1,2 units. The sample was dissolved in toluene and then poured into a round-shape flat Petri dish, 8 or 12 cm in diameter. The solution casting on a hot plate

* Corresponding author. Tel.: +81-75-724-7864; fax: +81-75-724-7800.
E-mail address: shin@ipc.kit.ac.jp (S. Sakurai).

0032-3861/02/$ - see front matter
PII: S0032-3861(02)00156-8

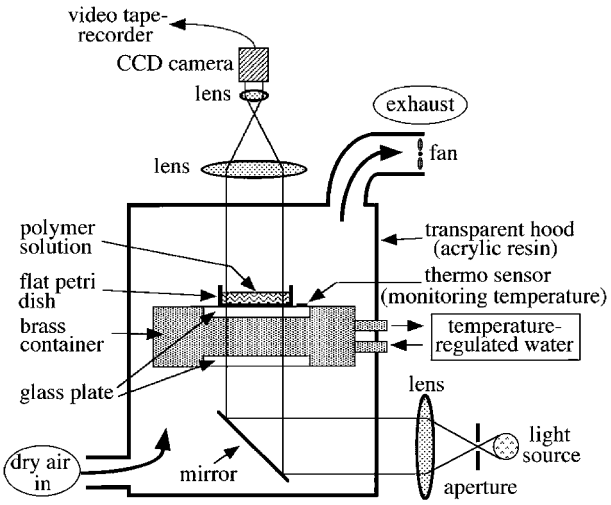

Fig. 1. Experimental set up for in situ observation of the process of imprinting convection pattern on a free surface of an as-cast polymer film as surface corrugation. It is consisted of an optical system, a temperature-regulated hot plate, and an isolated exhaust system for an organic solvent. The temperature of water in a reservoir was regulated and the temperature of the outer surface of the top glass plate was monitored by an adhesive thermocouple. The fan equipped at the exit of an exhaust pipe was used for control of the rate of solvent evaporation.

was conducted in the experimental set up shown in Fig. 1. Note that the important physical parameter relevant to this study is the density, which is 0.96 g/cm^3 for SBR-0202 and 0.868 g/cm^3 for toluene.

Fig. 1 shows a diagram of an experimental set up for in situ observation of imprinting process of a convection pattern on a free surface of an as-cast polymer film as surface corrugation. It is consisted of an optical system, a temperature-regulated hot plate, and an isolated exhaust system for an organic solvent. The optical system, which comprises a CCD camera (VH-5900, KEYENCE, Japan), lenses and a mirror, enables us to take the so-called shadowgraph [16] image in the course of solvent evaporation. The real time images were recorded with a video tape-recorder through the CCD camera. The temperature-regulated hot plate should be suited for the optical observation so that a circulation of temperature-regulated water was employed. The temperature of water in a reservoir was regulated and the temperature of the outer surface of the top glass plate was monitored by attaching an adhesive thermocouple. By calibration, the temperature of the polymer solution at the bottom of the Petri dish was evaluated. The isolated exhaust system was required because vapor of the organic solvent (toluene) spoils instruments of the optical system. In the meantime, it was especially needed for the present study in order to control the rate of solvent evaporation. The fan equipped at the exit of an exhaust pipe was used for this purpose. The hood is made of transparent acrylic resin for the optical observation.

In the present study, we discuss evaporation-rate dependence of the pattern imprinted on the surface of the as-cast film. The rate of solvent evaporation was evaluated by weighing a polymer solution for every 60 min. It was found that the weight of the solution linearly decreased with time until the concentration reached 90 wt% [9]. The evaporation-rate was hence determined from the slope.

The appearance of an as-cast polymer film was recorded on a photographic paper by shining light onto an as-cast film, which was piled on a photographic paper with an air gap of ca. 1 cm. The photographic records provide much higher resolution of images as compared to the video-tape recording.

3. Results and discussion

Fig. 2 displays temporal change in the pattern of the casting solution in the course of solvent evaporation. The initial polymer concentration was 15.0 wt% and the rate of solvent evaporation was 10.8 g/h for this particular case. The images (a)–(d) were taken, respectively, at 20, 60, 75, and 130 min elapsed from the onset of casting on a hot plate. Note here that the temperature of the polymer solution at the bottom of the Petri dish was 58.0 ± 1.0 °C. The polymer concentration was (a) 17, (b) 22, (c) 25, and (d)

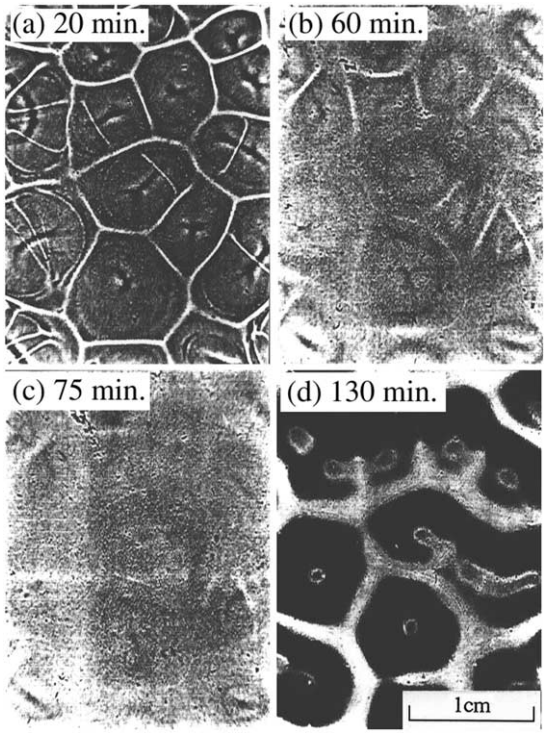

Fig. 2. Change in pattern of the casting solution with solvent evaporation. The initial polymer concentration was 15.0 wt% and the rate of solvent evaporation was 10.8 g/h for this particular case. The images (a) to (d) were taken, respectively, at 20, 60, 75, and 130 min elapsed from the onset of casting on a hot plate. The temperature of the polymer solution at the bottom of the Petri dish was 58.0 ± 1.0 °C. The polymer concentration was (a) 17.0, (b) 22.0, (c) 25.0, and (d) 48.0 wt%. The layer thickness of the solution, *d*, was evaluated to be (a) 3.2, (b) 2.5, (c) 2.2, and (d) 1.1 mm.

Table 1
Average mesh size ($\bar{D}$) and standard deviation for distribution of the mesh size (σ_D) evaluated from the images presented in Fig. 2, and the corresponding layer thickness of the solution (d), and the ratio $\bar{D}/d$

Time elapsed (min)	$\bar{D}$ (mm)	σ_D (mm)	d (mm)	$\bar{D}/d$
20	7.5	1.8	3.2	2.3
130	7.5	1.8	2.2	3.4

48 wt%. As discussed later, it is more important to know change in layer thickness of the solution, d, which was evaluated to be (a) 3.2, (b) 2.5, (c) 2.2, and (d) 1.1 mm. Note here that the values of d were calculated from its initial value (d_0) by taking account of the solvent evaporation-rate. The polygonal mesh pattern clearly observed in the image (a) is ascribed to active convection. The size of each mesh is in the range 7–8 mm, which is slightly larger than double the layer thickness of the solution at this moment (Table 1). Quantitative discussion on the size of the mesh pattern is made in the following paragraph. As the solvent evaporates, the polymer solution became viscous, which weakened the convection. Thus the polygonal mesh pattern in image (b) appears less obvious. At 75 min elapsed (c), the convection pattern completely disappeared, indicating cessation of convection because of high viscosity of the solution. However, it showed up again in image (d). The pattern is now ascribed not to convection but to surface corrugation. It was found that the surface was concave towards the central portion of a mesh-like cell. The imprinting mechanism of the convection pattern on a free surface of an as-cast polymer film as surface corrugation can be considered on the basis of the above results.

The mesh size was evaluated by measuring a distance (D) between centers of two-neighboring cells. For Fig. 2(a), some cells involve star-branched dark lines in their central regions and the branching point can be represented as the center. Since the mesh pattern was vague in image (b), it was difficult to accurately evaluate the mesh size. It is rather easy to specify the center of a cell in Fig. 2(d). The average mesh size ($\bar{D}$) and the standard deviation for its distribution (σ_D) is summarized in Table 1. Due to a limited number of cells in the restricted area shown in Fig. 2, the distribution of the cell separation is comparatively wide as is identified by the standard deviation σ_D being 24% of its average. Nevertheless, the average mesh size in Fig. 2(d) is found to be identical to that in Fig. 2(a). This result clearly indicates that the convection pattern has been precisely imprinted.

Fig. 3 shows schematic illustrations for change in side and through views of the casting solution. The through-view illustrations are idealized based on the above results and the side-view illustrations were drawn according to the following conjecture. In a dilute solution (a) where active convection is present, and in a semidilute solution (b) where the convection is almost inert, bright lines of the mesh are indicative of downflows of convection. Referring to the thermal (RB) convection, the size of the mesh can be scaled

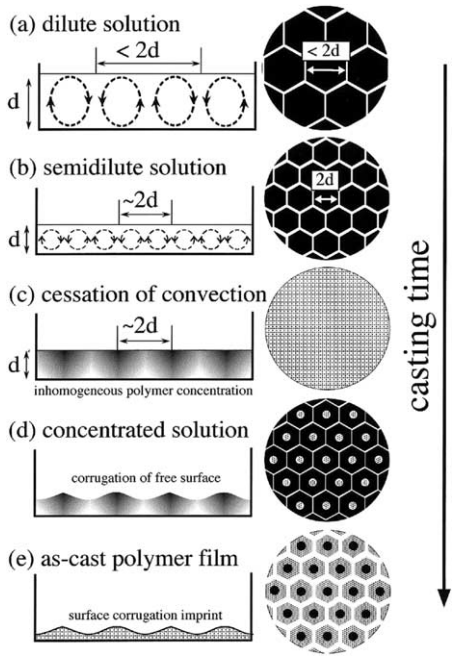

Fig. 3. Schematic illustrations for change in side and through views of a casting solution. The through-view illustrations are idealized based on the results shown in Fig. 2 and the side-view illustrations were drawn according to conjecture.

by the layer thickness of the convecting fluid at the onset of the RB convection. Namely, it equals approximately double the layer thickness [1–4]. On the other hand, the size of the mesh is less than that in the case when the convective flows are active. The mesh size found in Fig. 2(a) is in the range 7–8 mm, which is slightly larger than the double of the solution layer (Table 1). This fact implies that the convective flows cannot fully adjust the mesh pattern to the decrease in the layer thickness due to high viscosity.

It should be noted here that the convection in the casting solution can be ascribed to not only buoyancy but also surface tension, which is referred to as the BM convection. In this case, the surface of fluid is corrugated, which results in optical contrast giving rise to the polygonal mesh pattern, though the surface corrugation due to this effect is not schematically drawn in Fig. 3(a). Here, the upflow causes a hot spot on the surface. Considering the general temperature dependence of the surface tension, which is a decreasing function of temperature,[1] surrounding chillier surface drags the surface at the hot spot. Thus, the surface at the hot spot becomes concave and the surrounding surface becomes cusp, resulting in the bright mesh, meanwhile solvent evaporation takes latent heat away from the surface and lowers the surface temperature. Therefore, at such a portion, the surface temperature is lowered while the polymer solution is more concentrated and hence becomes

[1] Although surface tension of toluene does not exhibit a straightforward temperature dependency [17], that of water decreases monotonically with an increase of temperature [18].

heavier, resulting in downflows. Thus, the convective motion is stabilized. This is because the solute (polymer; SBR-0202) density is higher than the solvent (toluene) density. In a reverse case, a resulted lighter solution at the cooled surface destabilizes convective motion.

The solution at the downflow is heavier and that at the upflow is lighter. Such inhomogeneity in the polymer concentration is frozen-in in a solution even though the convection is ceased, as shown in Fig. 3(c). The residual inhomogeneous polymer concentration causes corrugation of the free surface in the successive solvent evaporation (Fig. 3(d)) when the polymer diffusion time is longer than the solvent evaporation time. Since the frozen inhomogeneity of the polymer concentration reflects the polygonal mesh pattern due to convection in the semidilute solution just before the cessation of convection, the forthcoming pattern in the successive casting process should be an imprint of the polygonal mesh pattern of convection. The highest concentration makes the surface convex and the lowest one makes it concave. Thus, the bright lines of the mesh in Fig. 2(d) are considered to be indicative of the surface cusp, and the central portion of each mesh should dent. Finally, the surface corrugation pattern is imprinted on the as-cast polymer film (Fig. 3(e)).

Above conjecture suggests that the rate of solvent evaporation can be an important control parameter for the surface corrugation pattern besides temperature of the hot plate. The typical results of evaporation-rate dependence are displayed in Fig. 4. It seems that the mesh size is decreased with an increase of the rate from (b) to (d). For quantitative comparison, a characteristic size of the mesh was evaluated using image analysis free software, the NIH image. Since the pattern near the side wall of the Petri dish was affected by its presence, a central square with $7.7 \times 7.7\ \mathrm{cm}^2$ area was extracted for the image analysis. Using the auto-correlation option of the NIH image, the corresponding two-dimensional auto-correlation function was obtained as shown in Fig. 5. Here, the level 0–255 in the gray scale corresponds to the degree of correlation (the darker indicates stronger correlation). Besides the strong correlation at the center of image, which is the self-correlation with $r = 0$, some other correlation spots are observed. Moreover, anisotropic patterns are observed because of their original anisotropic mesh patterns. Especially, as clearly seen in Fig. 5(b), approximately sixfold symmetric pattern indicates that each cell is surrounded by the six-nearest neighbors in the original pattern. Thus, the auto-correlation was found to be a useful tool to characterize the polygonal mesh pattern in this study. However, the anisotropic feature does not seem to be systematic with respect to the rate of solvent evaporation. Therefore, we only focus on the characteristic length (r^*).

To evaluate r^*, circular averaging of the two-dimensional pattern (Fig. 5) with respect to the center was conducted. Thus reduced one-dimensional auto-correlation function, $C(r)$, is now plotted in Fig. 6 as a function of the distance, r. The position of the first-order peak was taken as r^*. The same procedure was applied for all images and results are summarized in the plot of r^* vs. the rate of solvent evaporation in Fig. 7. Here, four different types of symbol are presented. The circles indicate results obtained for initial polymer concentration (c_0) of 10 wt%. Open and closed circles are results obtained, respectively, by using Petri dishes of 12 and 8 cm diameter. The closed square and the closed diamond show results for $c_0 = 7.5$ and 5.0 wt%,

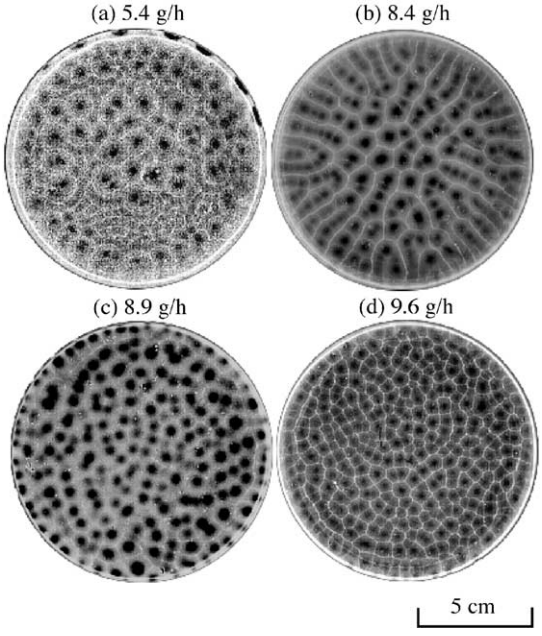

Fig. 4. Typical examples of an appearance of an as-cast polymer film by control of the rate of solvent evaporation.

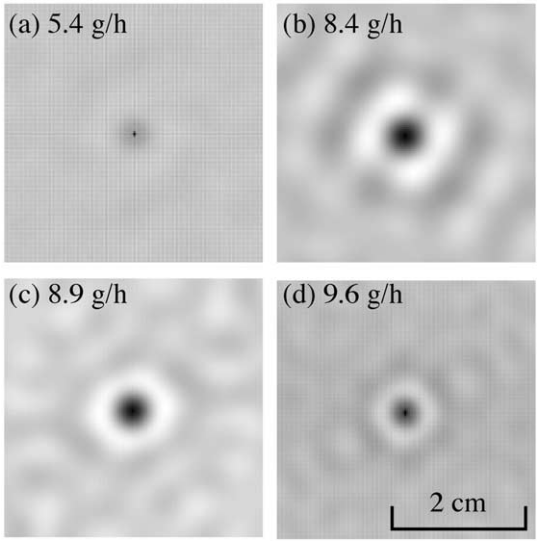

Fig. 5. Two-dimensional auto-correlation function for the images shown in Fig. 4 using image analysis free software, the NIH image. Since the pattern near the side wall of the Petri dish was affected by its presence, a central square with $7.7 \times 7.7\ \mathrm{cm}^2$ area of the original images in Fig. 4 was extracted for the image analysis. Here, the level 0–255 in the gray scale corresponds to the degree of correlation (the darker indicates stronger correlation).

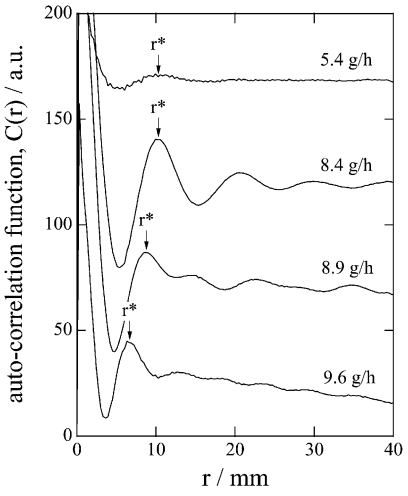

Fig. 6. One-dimensional auto-correlation function, $C(r)$, as a function of the distance, r. The position of the first-order peak was taken as the characteristic length, r^*.

respectively, with diameter of 12 cm. Note here that temperature of the casting solution at the bottom plate was 50.0 ± 1.0 °C (temperature of the hot plate was 57.0 °C) and that the final thickness of the as-cast polymer film was adjusted to about 0.4 mm for all cases. Albeit the difference in those experimental conditions, it seems that the results exhibit solely evaporation-rate dependence. Roughly speaking, the characteristic size exhibits increasing tendency in the lower evaporation-rate below 7.5 g/h (regime I), while steeply decreasing tendency above 7.5 g/h (regime II). This dual dependency can be interpreted as follows, based on the conjecture shown in Fig. 3.

In the regime I, the solvent evaporation is low so that the additional temperature-gradient due to cooling the solution surface by the solvent evaporation is negligible. In this case, the convection is caused by a genuine temperature-gradient across the casting solution on the hot plate. When the evaporation-rate is slow, the convective flows can adjust the mesh pattern to the decrease in the layer thickness of the solution. As the rate is accelerated, the adjustment is more or less kinetically prevented. In other words, the cessation of the convection is forwarded. Since the mesh size is determined by the layer thickness of the solution at the cessation of convection (Fig. 3(c)), the increase in the evaporation-rate results in the increase in r^*. Thus, the regime I can be referred to as a kinetic control regime. On the other hand, the cooling effect due to latent heat by active evaporation of the solvent governs the mechanism in the regime II. Namely, the temperature-gradient is enhanced with an increase in the rate and therefore the convective motion is more activated. The actively convecting flow delays its cessation, meanwhile the layer thickness is decreased. Thus, the mesh size at the cessation of the convection becomes smaller with the increase of the evaporation-rate. This scheme explains the decrease in r^* when the evaporation-rate in the regime II is increased. Hence, the regime II can be referred to as a temperature-gradient control regime.

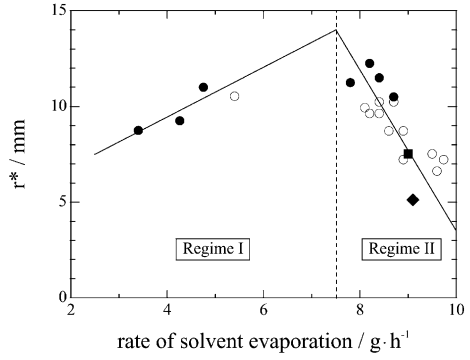

Fig. 7. Plot of the characteristic length r^* vs. the rate of solvent evaporation. Here, four different types of symbol are presented. The circles indicate results obtained for initial polymer concentration (c_0) of 10 wt%. Open and closed circles are results obtained, respectively, by using Petri dishes, 12 and 8 cm in diameter. The closed square and the closed diamond show results for $c_0 = 7.5$ and 5.0 wt%, respectively, with diameter of 12 cm. Note here that the temperature of the casting solution at the bottom plate was 50.0 ± 1.0 °C (temperature of the hot plate was 57.0 °C) and that the final thickness of the as-cast polymer film was adjusted to about 0.4 mm for all cases. The characteristic size exhibits increasing tendency in the lower evaporation-rate below 7.5 g/h (regime I), while steeply decreasing tendency above 7.5 g/h (regime II).

4. Conclusion

The imprinting mechanism of convection pattern on the as-cast polymer film as surface corrugation was studied by real time observation using the so-called shadowgraph technique for the solution casting of poly(styrene-*ran*-butadiene) random copolymer in toluene on a hot plate. Based on the mechanism, the control of the mesh size with the rate of solvent evaporation was considered. It was found that the mesh size was increased with an increase of the rate in the regime of the lower evaporation-rate (regime I) and that it was decreased tremendously with an increase of the rate in the regime of the higher evaporation-rate (regime II). These regimes can be referred to as a kinetic control regime and a temperature-gradient control regime, respectively.

Acknowledgements

This work was supported in part by the research grant from the Sumitomo Science Foundation (granted to S.S.).

References

[1] Chandrasekhar S. Hydrodynamic and hydromagnetic stability. New York: Dover, 1981.
[2] Manneville P. Dissipative structures and weak turbulence. Boston: Academic Press, 1990.
[3] Normand C, Pomeau Y, Verlade MG. Rev Mod Phys 1977;49:581.
[4] Cross MC, Hohenberg PC. Rev Mod Phys 1993;65:851.

[5] Assenheimer M, Steinberg V. Nature 1994;367:345.
[6] Ecke RE, Hu Y, Mainieri R, Ahlers G. Science 1995;269:1704.
[7] Seul M, Andelman D. Science 1995;267:476.
[8] Sakurai S, Tanaka K, Nomura S. Macromolecules 1992;25:7066.
[9] Sakurai S, Tanaka K, Nomura S. Polymer 1993;34:1089.
[10] Sakurai S, Tameno N, Nomura S. Forma 1993;8:309.
[11] Sakurai S. J Surf Sci Soc, Jpn 1997;18:549 (in Japanese).
[12] Sakurai S, Yoshida A, Furuhara S, Nomura S. Sen'i Gakkaishi 1998;54:491 (in Japanese).
[13] Furukawa C, Sakurai S, Ikkai F, Nomura S. Kobunshi Ronbunshu 1999;56:814 (in Japanese).
[14] Sakurai S, Wang Y, Kushiro T, Nambu T, Nomura S. Chem Phys Lett 2001;348:242.
[15] Widawski G, Rawiso M, François B. Nature 1994;369:387.
[16] Rasenat S, Hartung G, Winkler BL, Rehberg I. Exp Fluids 1989;7:412.
[17] Weast RC, editor. Handbook of chemistry and physics, 1st student ed. Boca Raton, Florida: CRC Press, 1988. p. F-17.
[18] Weast RC, editor. Handbook of chemistry and physics, 1st student ed. Boca Raton, Florida: CRC Press, 1988. p. F-14.